Annals of Pure and Applied Mathematics
Vol. 6, No. 1, 2014, 104-113
ISSN: 2279-087X (P), 2279-0888(online)
Published on 28 May 2014
www.researchmathsci.org

Effects of Porous Medium on MHD Fluid Flow along a Stretching Cylinder

R.S. Yadav[1] **and** ***P.R. Sharma***[2]
[1]Department of Mathematics, University of Rajasthan, Jaipur-302004, India
Email: rajendrauor@gmail.com
[2]Department of Mathematics, University of Rajasthan, Jaipur-302004, India
Email: profprsharma@yahoo.com

Received 12 April 2014; accepted 21May 2014

Abstract. Numerical solution of MHD fluid flow and heat transfer characteristics of a viscous incompressible fluid along a continuously stretching horizontal cylinder embedded in a porous medium was carried out in the presence of internal heat generation or absorption. The boundary layer equations with the convective boundary conditions were transferred into a system of non-linear ordinary differential equations and solved numerically by using fourth order Runge-Kutta integration scheme with shooting method. Numerical results obtained for velocity, temperature distributions, skin friction coefficient and Nusselt number. Characteristics of the flow and heat transfer for various values of the Prandtl number, stretching parameter and magnetic parameter analyzed and presented through graphs and tables.

Keywords: Porous medium, magnatohydrodynamic, stretching cylinder, heat transfer, boundary layer

AMS Mathematics Subject Classification (2010): 76A25

1. Introduction

The heat transfer due to free and mixed convection in fluid saturated porous media has been considered in many engineering problem such as MHD power generators, petroleum industries, plasma studies, geothermal system, heat insulation, drying technology, catalytic reactors, solar power collectors, food industries and many others. Many authors have been attracted to hydrodynamic flow and heat transfer over a stretching cylinders and flat plates due to its enormous applications in industries. Carne [1] reported flow past a stretching plate. Gupta [2] obtained heat and mass transfer on a stretching sheet with suction or blowing. Grubka and Bobba [3] obtained heat transfer characteristics of a continuous stretching surface with variable temperature. Sharma [4] obtained free convection effects on the flow of an ordinary viscous fluid past and infinite vertical porous plate with constant suction and constant heat flux. Aldos [5] discussed MHD mixed convection from a vertical cylinder embedded in a porous medium. Aldos and Ali [6] studied MHD free forced convection from a horizontal cylinder with suction and blowing. Ganesan and Rani [7] discussed unsteady free convection MHD flow past a vertical cylinder with heat and mass transfer. Bachok and Ishak [8] studied flow and heat transfer over a stretching cylinder with prescribed surface heat flux. Ali, Nazar, Arifin and Pop [9] obtained effect of Hall current on MHD mixed convection boundary layer flow over a stretched vertical flat plate. Abel, Tawade and Nandeppanavar [10] discussed MHD flow and heat transfer for the upper-convected Maxwell fluid over a stretching sheet.

The aim of the paper is to investigate boundary layer flow and heat transfer of a viscous and incompressible Newtonian fluid along a stretching cylinder in the presence of a constant transverse magnetic field and Variable surface temperature boundary condition.

2. Mathematical formulation

Consider the boundary layer flow due to free convection heat transfer from a horizontal cylinder of radius a and embedded in a porous medium saturated with a Newtonian fluid. It is assumed that the cylinder is stretched in the axial direction with linear velocity $u_w(x) = Ux/l$ and the surface of the cylinder is subjected to a variable temperature $T_w(x) = T_\infty + T_0(x/l)^n$. The x-axis is measured along the axis of the cylinder and y-axis is measured in the radial direction. A uniform magnetic field of strength B is acting in the radial direction. The magnetic Reynolds number is taken to be small enough such that the induced magnetic field is negligible. Under these assumptions and the boundary layer approximations, the governing equations are given by

$$\frac{\partial}{\partial x}(ru) + \frac{\partial}{\partial y}(rv) = 0, \tag{1}$$

$$u\frac{\partial u}{\partial x} + v\frac{\partial u}{\partial r} = \frac{\upsilon}{r}\frac{\partial}{\partial r}\left(r\frac{\partial u}{\partial r}\right) - \frac{\sigma B^2}{\rho}u - \frac{\upsilon}{K_p}u, \tag{2}$$

$$u\frac{\partial T}{\partial x} + v\frac{\partial T}{\partial r} = \frac{\alpha}{r}\frac{\partial}{\partial r}\left(r\frac{\partial T}{\partial r}\right) + \frac{Q}{\rho C_p}\left(T - T_\infty\right), \tag{3}$$

where u and v are the velocity components along the x and r directions, respectively. υ is the kinematic viscosity, σ is the electrical conductivity, ρ is the density of the fluid, K_p is the permeability of the porous medium, T is fluid temperature inside the thermal boundary layer, T_∞ is the fluid temperature in the free stream, α is the thermal diffusivity and Q is the volumetric rate of heat source or sink and C_p is the specific heat at constant pressure.

The boundary conditions are

$$r = a: \; u = u_w(x) = U\frac{x}{l}, \;\; v = 0, \;\; T = T_w(x) = T_\infty + T_0\left(\frac{x}{l}\right)^n$$

$$r \to \infty: \;\; u \to 0, \;\; T \to T_\infty \tag{4}$$

where U is the reference velocity, l is the characteristic length and T_0 is the reference temperature of the fluid. Introducing the following parameters and similarity variables

$$\eta = \frac{r^2 - a^2}{2a}\left(\frac{u_w}{\upsilon x}\right)^{1/2}, \quad \psi = (\upsilon x u_w)^{1/2} a f(\eta), \quad \theta(\eta) = \frac{T - T_\infty}{T_w - T_\infty}, \tag{5}$$

$$u = \frac{1}{r}\frac{\partial \psi}{\partial r}, \quad v = -\frac{1}{r}\frac{\partial \psi}{\partial x}$$

Into the equations (2) and (3), we get

$$\left(1 + 2\delta\eta\right) f''' + ff'' + 2\delta f'' - (f')^2 - \left(M + \beta\right) f' = 0, \tag{6}$$

$$\left(1 + 2\delta\eta\right)\theta'' + 2\delta\theta' + \Pr\left(f\theta' - nf'\theta\right) + \Pr S\theta = 0, \tag{7}$$

where ψ is the stream function, prime denotes differentiation with respect to η, $\delta\left\{= \left(\frac{\upsilon l}{a^2 U}\right)^{1/2}\right\}$ is the curvature parameter, $M\left\{= \frac{\sigma B^2 l}{\rho U}\right\}$ is the magnetic parameter, $\beta\left\{= \frac{\upsilon l}{U K_p}\right\}$ is the permeability parameter, $S\left\{= \frac{Ql}{U\rho C_p}\right\}$ is the heat generation parameter, $\Pr\left\{= \frac{\upsilon}{\alpha}\right\}$ is the Prandtl number, n is the surface temperature exponent.

It is noticed that equation (1) is identically satisfied. The boundary conditions are reduced to

$$f(0) = 0, \; f'(0) = 1, \; \theta(0) = 1, \; f'(\infty) \to 0, \; \theta(\infty) \to 0. \tag{8}$$

3. Skin friction Coefficient

The shearing stress at the surface is given by

$$\tau_w = \mu\left(\frac{\partial u}{\partial r}\right)_{r=a}, \tag{9}$$

where μ is the coefficient of viscosity.

The skin friction coefficient at the surface, is defined as

$$C_f = \frac{2\tau_w}{\rho u_w^2} \tag{10}$$

$$\Rightarrow \frac{1}{2} C_f \operatorname{Re}^{1/2} = f''(0), \tag{11}$$

where $\operatorname{Re}\left\{= \frac{lU}{\upsilon}\right\}$ is the Reynolds number.

4. Heat transfer Coefficient

The rate of heat transfer at the surface is given by

$$q_w = -\kappa\left(\frac{\partial T}{\partial r}\right)_{r=a}, \tag{12}$$

where κ is thermal conductivity of the fluid.

The Nusselt number is defined as

$$Nu_x = \frac{x}{\kappa}\frac{q_w}{\left(T_w - T_\infty\right)} \tag{13}$$

$$\Rightarrow \frac{Nu_x}{\operatorname{Re}^{1/2}} = -\theta'(0). \tag{14}$$

The governing non-linear boundary layer equations (6) and (7) are solved numerically using Runge- Kutta fourth order integration scheme with shooting integration technique. The effects of physical parameters on the velocity and temperature profiles are shown through graphs. The numerical values of skin friction and heat transfer coefficients are derived for different values of physical parameters and presented through Tables.

5. Results and discussion

It is seen from figure 1 that as M increases, the velocity profiles decrease. As M increases, the Lorentz force which opposes the flow also increases leads to enhance deceleration of the flow. Figure 2 depicts that fluid velocity profiles decrease due to increase in permeability parameter which agrees with natural phenomena. Figure 3 indicates the influence of the curvature parameter on velocity profiles. It is observed that velocity profiles increases as curvature parameter increases. It is seen from figure 4 that thermal boundary layer thickness increases with increasing values of the magnetic parameter. It is noted from Figure 5 that as permeability parameter increases, the temperature decreases. The temperature profiles increase as the curvature parameter increases as seen from figure 6. It is observed from figure 7 that thermal boundary layer thickness decreases with the increase of Prandtl number. From a physical point of view, if Prandtl number increases, the thermal diffusivity decreases and this phenomenon lead to the decreasing of energy ability that reduces the thermal boundary layer. Figure 8 depicts, that as heat generation parameter increases, the temperature profiles increase. It is seen from figure 9 that as surface temperature exponent increases, the temperature profiles decrease. In order to validate the method used in this study and to judge the accuracy of the present analysis, the numerical values of skin friction coefficient and heat transfer coefficient for the stretching cylinder are compared with those of Gurbka [1985], Ali et al [2011], Abel et al [2012]. A good agreement is observed between these results shown in Table 1 and Table 2, which lends confidence in the numerical results to be reported subsequently.

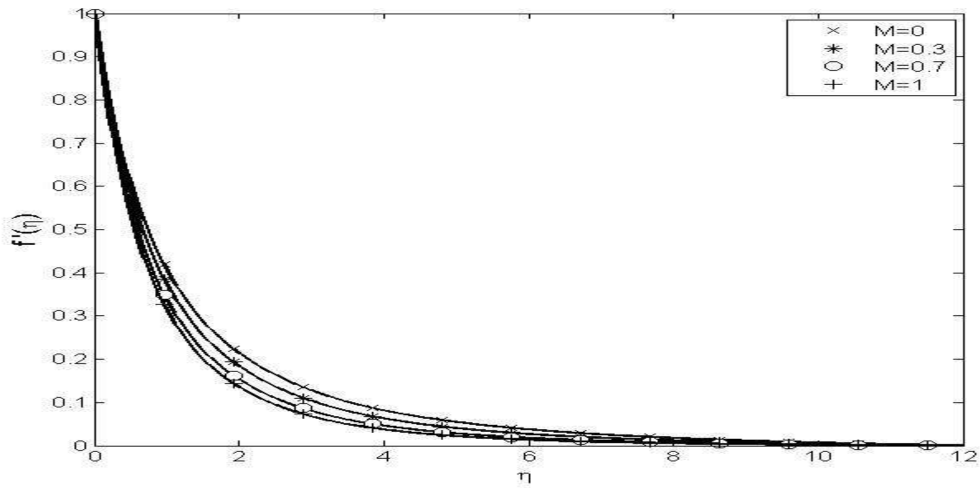

Figure 1: Velocity distribution versus η when $\Pr = 7, S = 0.5, n = 0.5, \beta = 0.5, \delta = 0.5$.

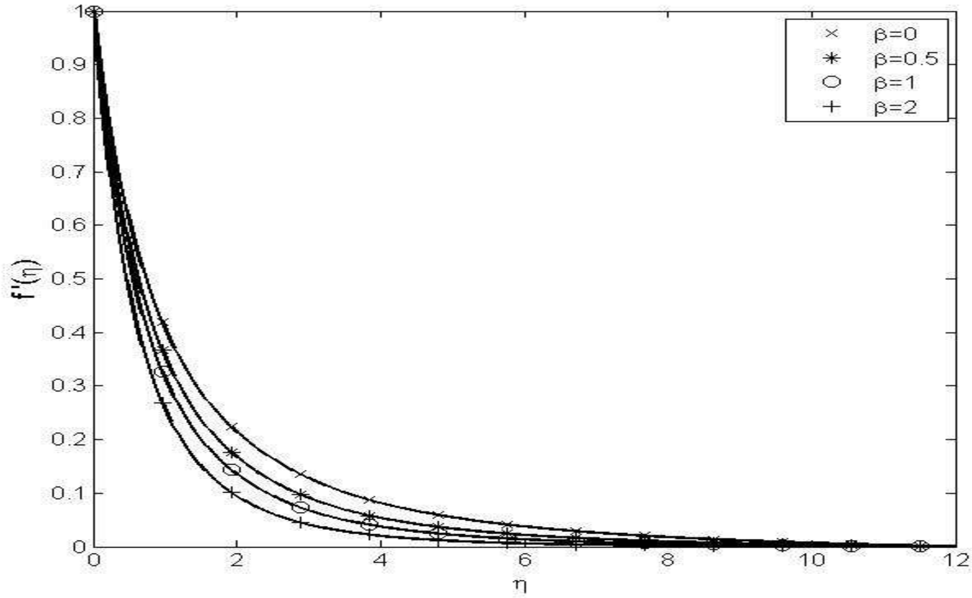

Figure 2: Velocity distribution versus η when $\Pr = 7, S = 0.5, M = 0.5, n = 0.5, \delta = 0.5.$

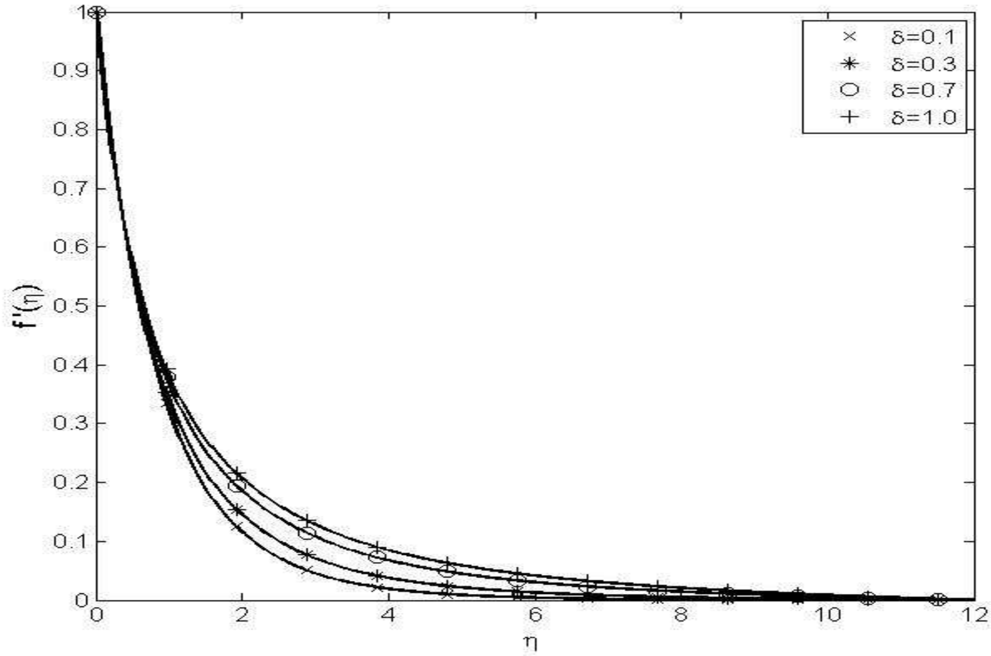

Figure 3: Velocity distribution versus η when $\Pr = 7, S = 0.5, M = 0.5, n = 0.5, \beta = 0.5.$

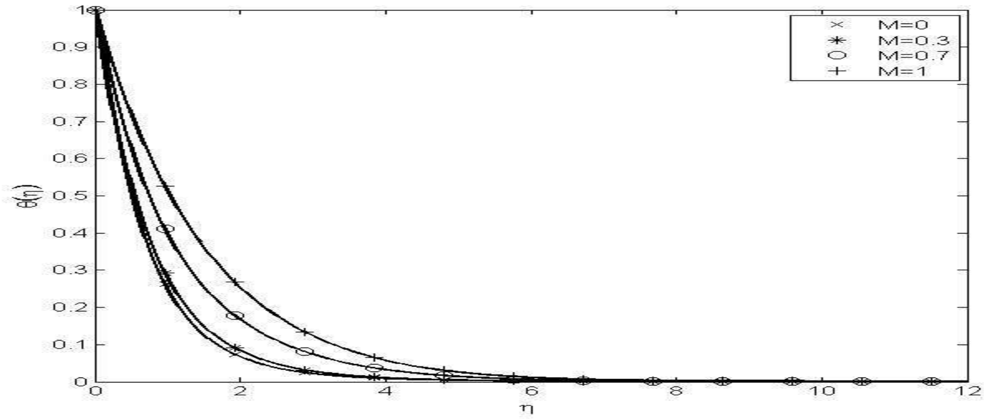

Figure 4: Temperature distribution versus η when $\Pr = 7, S = 0.5, n = 0.5, \beta = 0.5, \delta = 0.5.$

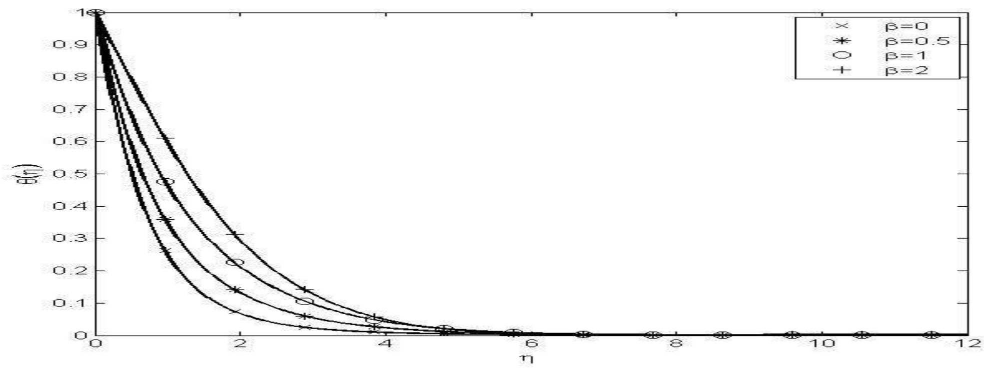

Figure 5: Temperature distribution versus η when $\Pr = 7, S = 0.5, M = 0.5, n = 0.5, \delta = 0.5.$

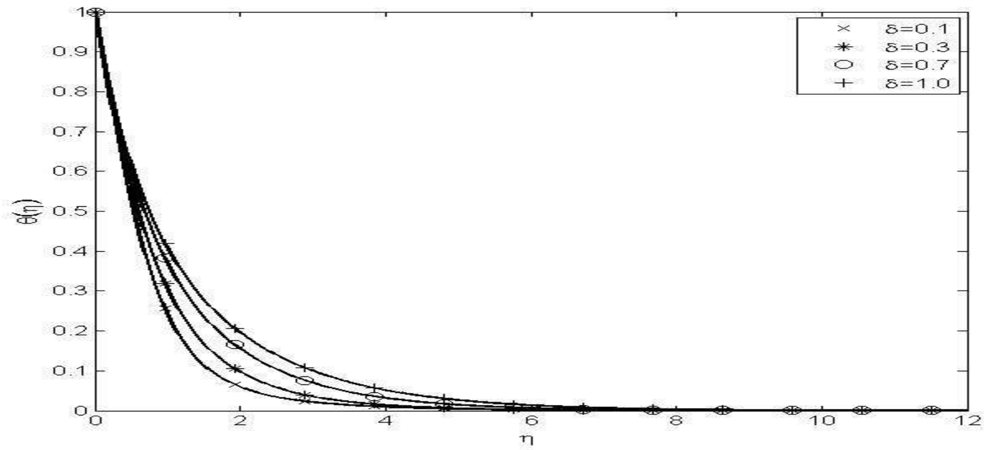

Figure 6: Temperature distribution versus η when $\Pr = 7, S = 0.5, M = 0.5, n = 0.5, \beta = 0.5.$

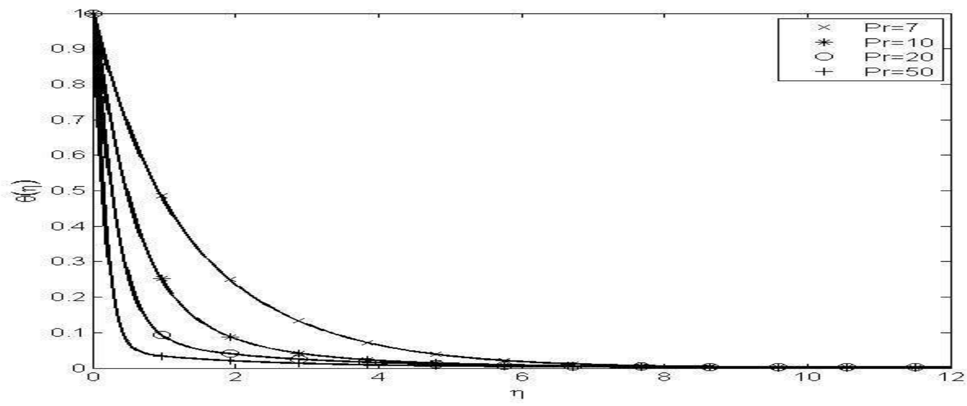

Figure 7: Temperature distribution versus η when $S = 0.5, M = 0.5, n = 0.5, \beta = 0.5, \delta = 0.5.$

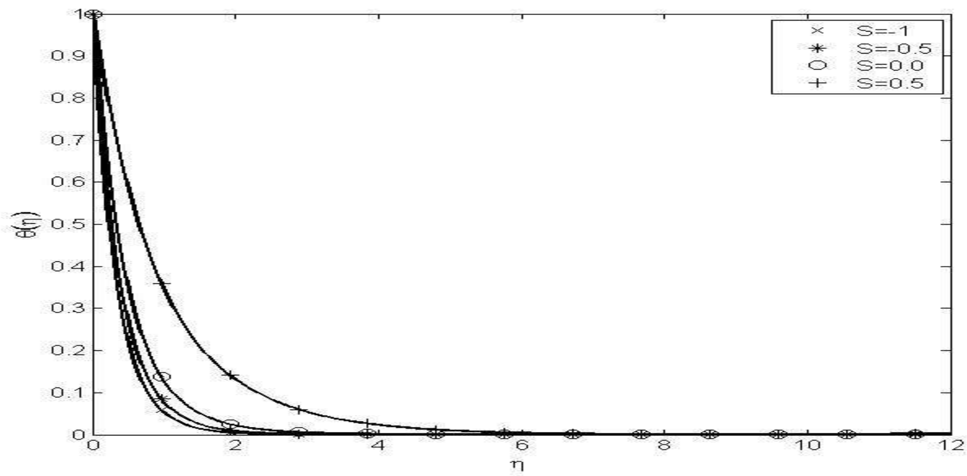

Figure 8: Temperature distribution versus η when $\Pr = 7, M = 0.5, n = 0.5, \beta = 0.5, \delta = 0.5.$

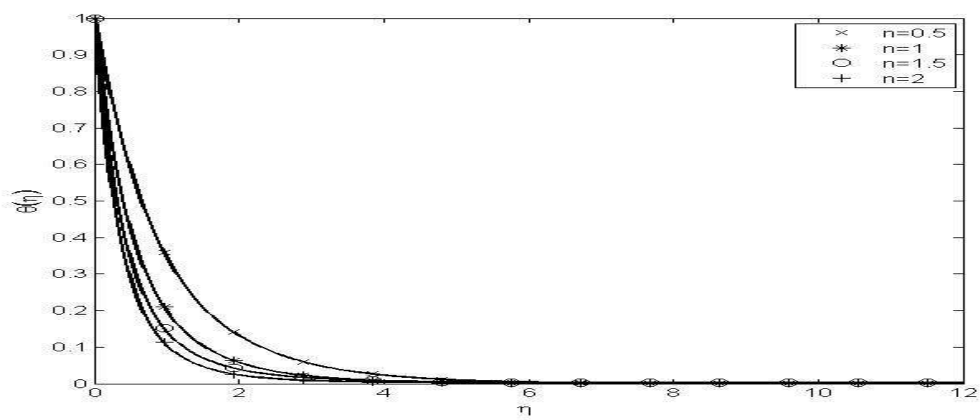

Figure 9: Temperature distribution versus η when $\Pr = 7, S = 0.5, M = 0.5, \beta = 0.5, \delta = 0.5.$

Table 1: Comparison of numerical values of $f''(0)$ for various values of M for stretching cylinder with $\beta = 0$ and $\delta = 0$.

M	Abel et al [2012]	Present study
0.0	-0.999962	0.999962
0.2	-1.095445	-1.095445

Table 2: Comparison of numerical values of $-\theta'(0)$ for various values of Pr and n with $S = 0, M = 0, \beta = 0, \delta = 0$.

Pr	n	Grubka [1985]	Ali et al [2011]	Abel et al [2012]	Present study
0.72	1	0.8086	0.8086	-	0.808689
1	1	1.0000	1.0000	1.000174	1.000000
3	-1	0.0	-	-	-0.038721
3	0	1.1652	-	-	1.154551
3	1	1.9237	1.9237	1.923609	1.923700
3	2	2.5097	-	-	2.515901
10	-1	0.0	-	-	-0.080751
10	0	2.3080	-	-	2.299989
10	1	3.7207	3.7208	-	3.719976
10	2	4.7969	-	-	4.808102

Table 3: Numerical values of skin friction coefficient and Nusselt number at the surface for various values of physical parameters.

Pr	S	n	β	M	δ	$-f''(0)$	$-\theta'(0)$
20	0.5	0.5	0.5	0.5	0.5	1.568286	2.146312
50	0.5	0.5	0.5	0.5	0.5	1.568286	4.485325
100	0.5	0.5	0.5	0.5	0.5	1.568286	6.985691
7	-0.5	0.5	0.5	0.5	0.5	1.568286	3.227012

7	0.0	0.5	0.5	0.5	0.5	1.568286	2.523121
7	0.5	0.5	0.5	0.5	0.5	1.568286	1.023121
7	0.5	1.0	0.5	0.5	0.5	1.568286	1.823197
7	0.5	1.5	0.5	0.5	0.5	1.568286	2.703146
7	0.5	0.5	1.0	0.5	0.5	1.741353	1.203760
7	0.5	0.5	1.5	0.5	0.5	1.896457	1.137402
7	0.5	0.5	2.0	0.5	0.5	2.038344	0.800740
7	0.5	0.5	0.5	0.0	0.5	1.368981	1.168357
7	0.5	0.5	0.5	0.3	0.5	1.492376	1.170740
7	0.5	0.5	0.5	0.7	0.5	1.640082	1.185342
7	0.5	0.5	0.5	0.5	0.3	1.509707	1.003791
7	0.5	0.5	0.5	0.5	0.7	1.623808	1.064235
7	0.5	0.5	0.5	0.5	1.0	1.702086	1.104235

6. Conclusion

Steady two dimensional MHD boundary layer flow of an incompressible viscous fluid over a stretching cylinder is investigated with heat source or sink is placed within the flow to allow for possible heat generation or absorption effects. Numerical calculations are carried out for various values of the physical parameters and the following conclusions are made:

- (i) Fluid velocity profiles decrease due to increase in the magnetic parameter and permeability parameter.
- (ii) Fluid velocity profiles increase due to increase in curvature parameter.
- (iii) Fluid temperature decreases due to increase in surface temperature exponent or Prandtl number.
- (iv) Fluid temperature increases due to increase in permeability parameter, magnetic parameter, heat generation parameter or curvature parameter.
- (v) Skin friction coefficient and Nusselt number both increase with the increase of magnetic parameter.
- (vi) Nusselt number increases with the increase of Prandtl number, surface temperature exponent or curvature parameter, but it decreases due to increase of heat generation parameter or permeability parameter.

REFERENCES

1. L.J. Carne, Flow past a stretching plate, *Z. Angew. Math. Phys.*, 21 (1970) 645-647.
2. P.S. Gupta, Heat and mass transfer on a stretching sheet with suction or blowing, *Can. J. Chem. Eng*., 55 (1977) 744-746.
3. L.J. Grubka and K.M. Bobba, Heat transfer characteristics of a continuous stretching surface with variable temperature, *Journal of Heat Transfer*, 107 (1985) 248-250.
4. P.R. Sharma, Free convection effects on the flow of an ordinary viscous fluid past and infinite vertical porous plate with constant suction and constant heat flux. *J. Ult. Scientist. Phyl. Sciences*, 3 (1991) 88-91.
5. T.K. Aldos, MHD mixed convection from a vertical cylinder embedded in a porous medium, *Int. Comm. Heat Mass Transfer*, 23(4) (1996) 517-530.
6. T.K. Aldos and Y.D. Ali, MHD free forced convection from a horizontal cylinder with suction and blowing, *Int. Comm. Heat Mass Transfer*, 24(5) (1997) 689-693.
7. P.G. Ganesan and P.H. Rani, Unsteady free convection MHD flow past a vertical cylinder with heat and mass transfer, *Int. J. Therm. Sci*., 39 (2000) 265-272.
8. N. Bachok and A. Ishak, Flow and heat transfer over a stretching cylinder with prescribed surface heat flux, *Malaysian Journal of Mathematical Sciences*, 4(2) (2010) 159-169.
9. F.M. Ali, R. Nazar, N.M. Arifin and I. Pop, Effect of Hall current on MHD mixed convection boundary layer flow over a stretched vertical flat plate, *Meccanica*, 46 (2011) 1103-1112.
10. M.S. Abel, J.N. Tawade and M.M. Nandeppanavar, MHD flow and heat transfer for the upper-convected Maxwell fluid over a stretching sheet, *Meccanica*, 47 (2012) 385-393.